

# Rho Kinase Inhibitor AR-12286 Reverses Steroid-Induced Changes in Intraocular Pressure, Effective Filtration Areas, and Morphology in Mouse Eyes

Ruiyi Ren,<sup>1</sup> Anne A. Humphrey,<sup>1</sup> Casey Kopczynski,<sup>2</sup> and Haiyan Gong<sup>1</sup>

<sup>1</sup>Boston University School of Medicine, Department of Ophthalmology, Boston, Massachusetts, United States

<sup>2</sup>Aerie Pharmaceuticals, Inc., Durham, North Carolina, United States

Correspondence: Haiyan Gong, Department of Ophthalmology, Boston University School of Medicine, 72 East Concord Street, Room L-905, Boston, MA 02118, USA; [hgong@bu.edu](mailto:hgong@bu.edu).

**Received:** September 3, 2022

**Accepted:** January 11, 2023

**Published:** February 3, 2023

Citation: Ren R, Humphrey AA, Kopczynski C, Gong H. Rho kinase inhibitor AR-12286 reverses steroid-induced changes in intraocular pressure, effective filtration areas, and morphology in mouse eyes. *Invest Ophthalmol Vis Sci.* 2023;64(2):7. <https://doi.org/10.1167/iovs.64.2.7>

**PURPOSE.** We investigated mechanisms of reduction of intraocular pressure (IOP) by Rho kinase inhibitor AR-12286 in steroid-induced ocular hypertension (SIOH).

**METHODS.** C57BL/6 mice (N = 56) were randomly divided into Saline, dexamethasone (DEX), DEX + AR-12286, and DEX-discontinuation (DEX-DC) groups. IOP was measured weekly during the first four weeks in all groups. Beginning at week 5, the DEX-DC group was followed without treatment until IOP returned to normal, and the other groups were treated as assigned with IOP measured every other day for another week. Fluorescent tracer was injected into the anterior chamber to visualize the outflow pattern in the trabecular meshwork (TM) and TM effective filtration area (EFA) was determined. Radial sections from both high- and low-tracer regions were processed for electron microscopy.

**RESULTS.** AR-12286 reduced IOP in SIOH mouse eyes in one day ( $P < 0.01$ ). At the end of week 5, mean IOP in the DEX + AR-12286 group was ~4 mm Hg lower than DEX group ( $P < 0.001$ ) and ~2 mm Hg lower than DEX-DC group ( $P < 0.05$ ). After one-week AR-12286 treatment ( $P < 0.05$ ) or five-week DC of DEX ( $P < 0.01$ ), DEX-induced reduction of EFA was rescued and DEX-induced morphological changes in the TM were partially reversed.

**CONCLUSIONS.** AR-12286 reversed steroid-induced morphological changes in the TM and reduced EFA, which correlated with reduced IOP in SIOH eyes. AR-12286 reduced IOP elevation in SIOH eyes more effectively than discontinuing DEX treatment even when accompanied by continuous DEX treatment. Therefore Rho kinase inhibitors may lower SIOH in patients who rely on steroid treatment.

**Keywords:** rho kinase inhibitor, AR-12286, steroid-induced ocular hypertensive mouse model, effective filtration area, trabecular meshwork, intraocular pressure, morphology, confocal microscopy, transmission electron microscopy

Elevated intraocular pressure (IOP), resulting from increased resistance to aqueous humor outflow, is a major risk factor for the development and progression of glaucoma, a leading cause of blindness worldwide.<sup>1,2</sup> Many studies have proven that reduction of IOP in glaucoma can slow damage to the optic nerve and preserve vision.<sup>3-8</sup> Reduction of IOP via medical, laser, or surgical means remains the sole clinical objective for the treatment of this blinding disease.<sup>9,10</sup>

In glaucomatous eyes, elevation of IOP results from an abnormally increased resistance to outflow in the trabecular outflow pathway. The causes of this increased outflow resistance are not fully understood, but current evidence supports an increase in the contractile tone and stiffness of the trabecular meshwork (TM), changes in extracellular matrix (ECM) composition and/or a decrease in the conductance of the inner wall (IW) of Schlemm's canal (SC).<sup>11-18</sup> In the TM, experimental evidence suggests that the majority of outflow resistance is generated in the juxtacanalicular

connective tissue (JCT) region<sup>2,19,20</sup> and is modulated by the IW endothelial cells of SC and their pores.<sup>21,22</sup>

Previous tracer studies concluded that aqueous humor outflow through the TM and into SC is "segmental" rather than uniform.<sup>23-34</sup> We termed the active fraction of the total area of the outflow pathway as effective filtration area (EFA),<sup>29</sup> which was previously analyzed by measuring percent effective filtration length (PEFL). Our group found a positive correlation between PEFL and outflow facility across three species (bovine, monkey, and human) with marked differences in the morphology of their outflow pathways, especially in the TM.<sup>24,28,35,36</sup> Furthermore, a negative correlation was found between the TM PEFL and IOP in both a genetic ocular hypotensive mouse model<sup>37</sup> and a steroid-induced ocular hypertensive mouse model,<sup>38</sup> with correlated morphological changes found in the TM.

The newest class of ocular hypotensive drugs, Rho kinase (ROCK) inhibitors, serves to decrease IOP by inhibiting ROCK, a serine/threonine kinase whose activity increases

actomyosin contraction in smooth muscle-like cells, including the myofibroblast-like cells of the TM. Rho kinase inhibitors have been shown to relax the overall tone of the contractile cells in TM,<sup>17,39–42</sup> alter tissue architecture in such a way that expands the JCT region,<sup>17,28,36</sup> and increase the permeability of cultured SC cell monolayers.<sup>17</sup> Previous studies had shown that ROCK/NET (norepinephrine transporter) dual inhibitor netarsudil, a novel glaucoma medication used in patients with glaucoma or ocular hypertension (OHT), lowers IOP primarily by increasing outflow through the TM in addition to decreasing both aqueous humor production and episcleral venous pressure.<sup>30,36,43–45</sup> Our study in ex vivo human donor eyes demonstrated increased EFA with correlated morphological changes in the TM after netarsudil perfusion.<sup>36</sup> Other studies had shown that netarsudil may decrease IOP and increase outflow facility in both normotensive<sup>30</sup> and steroid-induced ocular hypertensive (SIOH) mouse eyes,<sup>45,46</sup> with morphological and stiffness changes found in the TM, especially in the JCT region. Increased fluorescent microbeads distribution was also found in normotensive mouse eyes with in vivo perfusion after netarsudil treatment.<sup>30</sup> All these findings suggest that it is possible for the ROCK inhibitor to reduce IOP by restoring the steroid-induced morphological changes in the TM and increasing EFA in SIOH eyes.

Although the long-term usage of steroids can cause elevation of IOP, steroids remain the main therapy for inflammatory and immune-mediated diseases, and their usage may be necessary for patients with life-threatening cases, such as kidney inflammation, or vision-impairing cases, such as macular edema and uveitis. Therefore, although in most cases the SIOH is reversible, the cessation of steroid treatment may not be practical for some patients. Until effective alternatives to nonsteroidal anti-inflammatory therapies are developed, there is still a need to optimize therapy for those patients relying on steroid treatment. Netarsudil has previously been shown to lower IOP in steroid-induced glaucoma patients whose OHT was poorly controlled by standard glaucoma medications.<sup>45</sup>

To investigate the mechanisms of SIOH, our lab recently reported a hydrodynamic and morphological comparison study by using a dexamethasone (DEX)-induced ocular hypertensive mouse model.<sup>38</sup> Our data suggested that topical DEX treatment increases IOP in mouse eyes by reducing the EFA in the TM. Morphological correlations with the reduction of EFA include compacting the JCT in high tracer regions and abnormal accumulation of ECM in the TM, including basement membrane (BM)-like materials, fingerprint-like arranged materials resembling basement membrane (FBM), short curly filaments, and more continuous BM of the IW of SC. Similar ECM changes have been reported in SIOH human and animal eyes.<sup>47–51</sup>

AR-12286 is a highly selective ROCK inhibitor developed by the same company as netarsudil (Aerie Pharmaceuticals, Inc., Durham, NC, USA), but with no NET activity and less off-target kinase activity.<sup>52,53</sup> In previous clinical trials, it has been shown to lower IOP in patients with glaucoma or OHT within one week, with the best IOP reduction effect produced by 0.25% AR-12286 after twice daily dosing.<sup>54,55</sup> In the current study, we explored whether the ROCK inhibitor AR-12286 can rescue SIOH and offset the DEX-induced changes in the trabecular outflow pathway and whether these effects are comparable to the effects produced by the discontinuation of steroid administration.

## METHODS

### Animal Husbandry

All experiments were completed in compliance with the Association for Research in Vision and Ophthalmology Statement for the Use of Animals in Ophthalmic and Vision Research. Local Institutional Animal Care and Use Committee approval was obtained. Fifty-six C57BL/6 mice (6-week-old) were purchased from Charles River Laboratories (Wilmington, MA, USA). All mice were housed in the Animal Science Center of Boston University Medical Campus, with a 12-hour light/12-hour dark cycle and access to food and water as desired. On arrival, mice were examined to confirm a normal appearance (i.e., free of any signs of ocular disease) and allowed to acclimatize for at least three days before experiments.

### Eye Drops Administration

Fifty-six mice were randomly divided into four groups: Saline, DEX, DEX + AR-12286, and discontinuation of DEX (DEX-DC). The composition and detailed treatments of each group are shown in Tables 1 and 2, respectively. A small eye drop (~10  $\mu$ L) of either 0.1% dexamethasone phosphate (Henry Schein Inc., Melville, NY, USA) (DEX, DEX + AR-12286, and DEX-DC groups) or sterile saline solution (Teknova Inc. Hollister, CA) (Saline group) (both containing 9.4 mg/mL hydroxyethyl cellulose) was topically applied to both eyes of each mouse under light anesthesia (isoflurane) twice per day for four weeks. At week 5, the Saline group was treated with saline solution four times a day. The DEX group was treated with two doses of saline solution in addition to the two doses of dexamethasone treatment each day, whereas the DEX + AR-12286 group was treated with two doses of dexamethasone and two doses of 0.25% AR-12286. The DEX-DC group did not receive any treatment after four weeks.

### IOP Measurement

IOP was measured in all groups at baseline and then weekly between 8 AM and 10 AM for four weeks (before the application of the first dose of eye drops) using a rodent rebound tonometer (Icare TONOLAB; Icare, Vantaa, Finland) with constant flow of 2.5% isoflurane (Henry Schein Inc.). The measurement procedure was described in detail in our previous study.<sup>38</sup> At week 5, for the Saline, DEX, and DEX+AR-12286 groups, IOP was measured on day 0 (week 5 baseline), 1, 3, 5 and 7. For DEX-DC group, IOP was measured weekly from week 5 until it returned to a similar level as the Saline group (around week 9, five weeks after DC of DEX). Because each eye responds differently to treatment, each eye was measured as an independent data point for IOP.<sup>38,56</sup>

TABLE 1. Number of Mice and Sex Distribution in Each Group

Group	Number of Mice	Sex Distribution
Saline	15	8 females + 7 males
DEX	16	8 females + 8 males
DEX + AR-12286	14	8 females + 6 males
DEX-DC	11	5 females + 6 males

TABLE 2. Daily Treatments for Each Group

Group	Week 1–4		Week 5				Week 6–9
	8:00–10:00 AM	2:30–4:30 PM	8:00–10:00 AM	11:00 AM–12:30 PM	2:30–4:30 PM	5:30–7:00 PM	
Saline	Saline	Saline	Saline	Saline	Saline	Saline	—
DEX	DEX	DEX	DEX	Saline	DEX	Saline	—
DEX + AR-12286	DEX	DEX	DEX	AR-12286	DEX	AR-12286	—
DEX-DC	DEX	DEX	Discontinuation of DEX treatment				—

### Tracer Injection

At the end of the experiment (end of week 5 for Saline, DEX, and DEX+AR-12286 groups; week 9 for DEX-DC group), one eye of each mouse was then injected with fluorescent tracers as previously described.<sup>37,38</sup> In brief, 1  $\mu$ L solution of 20 nm tracers (Ex/Em: 505/515, 2%; Invitrogen, Carlsbad, CA, USA) diluted 1:50 in Dulbecco's phosphate-buffered saline solution (v/v) was injected into the anterior chamber of mouse eyes at 4 nL/s by a microprocessor-based microsyringe pump controller (Micro4; World Precision Instruments, Sarasota, FL, USA). After the injection was completed, 45 minutes were allowed for the tracers to migrate through the anterior chamber, penetrate the TM, and reach SC, while the needle remained in the eye. During this time, artificial tears (Henry Schein Inc.) were applied to the cornea of both eyes to prevent dehydration. To prevent blood reflux into SC when the needle was withdrawn, modified Karnovsky's fixative (2  $\mu$ L) was subsequently injected into the anterior chamber while additional fixative was simultaneously applied to the exterior of the eye for 30 minutes. Both eyes were enucleated after euthanasia of the mouse, fixed in Karnovsky's fixative, then transferred in phosphate-buffered saline solution, and kept at 4°C for further processing. The 12 o'clock position of the eye was marked to provide orientation.

### Confocal Microscopy

All tracer-injected eyes were examined using an Olympus MVX10 (Olympus, Tokyo, Japan) fluorescent stereomicroscope. Eyes with no tracer present in the TM region were excluded from further processing and analyses. Each of the successfully injected eyes (Saline: n = 11; DEX: n = 11; DEX + AR-12286: n = 7; DEX-DC: n = 6) were dissected into eight radial "wedges" as described previously.<sup>38</sup> For trabecular outflow imaging, each wedge was immersed in mounting media (Life Technologies, Carlsbad, CA, USA) in a glass-bottom dish and imaged in the en face view from the corneal side with a Zeiss LSM 700 confocal microscope (Carl Zeiss, Peabody, MA, USA). The images were taken with a  $\times$ 10 objective and maximum pinhole (confocal slice thickness = 143  $\mu$ m), to capture the entire fluorescence throughout the thickness of the TM tissue. Images were captured using the ZEN2010 operating software (Carl Zeiss).

Two radial sections were obtained from high- and low-tracer regions respectively (four radial sections in total) of each eye. The obtained radial sections were confirmed as regions with high or low tracer distribution in the TM using confocal microscopy.

### PEFL Analysis

In the trabecular outflow images of each radial wedge, "total length" of the TM (TL) and "filtration length" of TM contain-

ing tracer (FL) were measured using ZEN blue 2.3 imaging software (Carl Zeiss) with white balance set at 120, computer monitor resolution set at 1920  $\times$  1080. The average percent effective filtration length (TM PEFL =  $\Sigma$ FL/ $\Sigma$ TL  $\times$  100%) in each eye was subsequently calculated as performed in previous studies (Fig. 1A).<sup>29,36–38</sup>

### Light and Electron Microscopy

Radial sections with high- or low-tracer presence confirmed by confocal microscopy in 5–6 randomly selected eyes (five for DEX-DC group and six for all other groups) from each group were processed for light and electron microscopy. Sections were post-fixed with 2% osmium tetroxide in 1.5% potassium ferrocyanide for two hours, en bloc stained with 1.5% uranyl acetate for 90 minutes, dehydrated in an ascending series of ethanol and propylene oxide, and embedded in Epon-Araldite. After semithin sections (1  $\mu$ m) were cut and examined with light microscopy, sections containing regions of interest were then prepared for electron microscopy (at least one radial section from high- and low-tracer regions was imaged using electron microscopy in each randomly-selected eye); ultrathin sections (80 nm) were obtained, stained with 4% methanol-based uranyl acetate to visualize extracellular matrix, and examined using a transmission electron microscope (JEOL JEM-1010, Tokyo, Japan). Images were taken along SC at original magnifications  $\times$ 3000,  $\times$ 5000, and  $\times$ 10,000.

### Measurements of PBML of the IW of SC

Percentage BM length (PBML) of the IW of SC was measured by using  $\times$ 3000 TEM images of radial sections from high- and low-tracer regions. The IW length and length of BM was measured as shown in Figure 1B. PBML was calculated as  $\Sigma$  length of BM/ $\Sigma$  IW length  $\times$  100%. At least 50  $\mu$ m of IW length was analyzed in each section. The overall PBML for each eye was estimated by using TM PEFL as  $PBML_{overall} = PBML_{high\ tracer\ region} \times TM\ PEFL + PBML_{low\ tracer\ region} \times (1 - TM\ PEFL)$ .

### Measurements of the JCT Thickness

JCT area was measured in electron microscopic images of radial sections ( $\times$ 3000) by selecting the area from the basal side of the IW endothelium to the empty space adjacent to the outermost corneoscleral beams and measuring the cross-sectional area using ImageJ. JCT length was also measured by ImageJ. JCT thickness was then calculated (Fig. 1C). Only the images showing a clear outermost beam were used for JCT thickness measurements. At least 30  $\mu$ m length of JCT was measured for each section. The JCT thickness of each group is the mean of the radial sections of five to six eyes. The overall JCT thick-

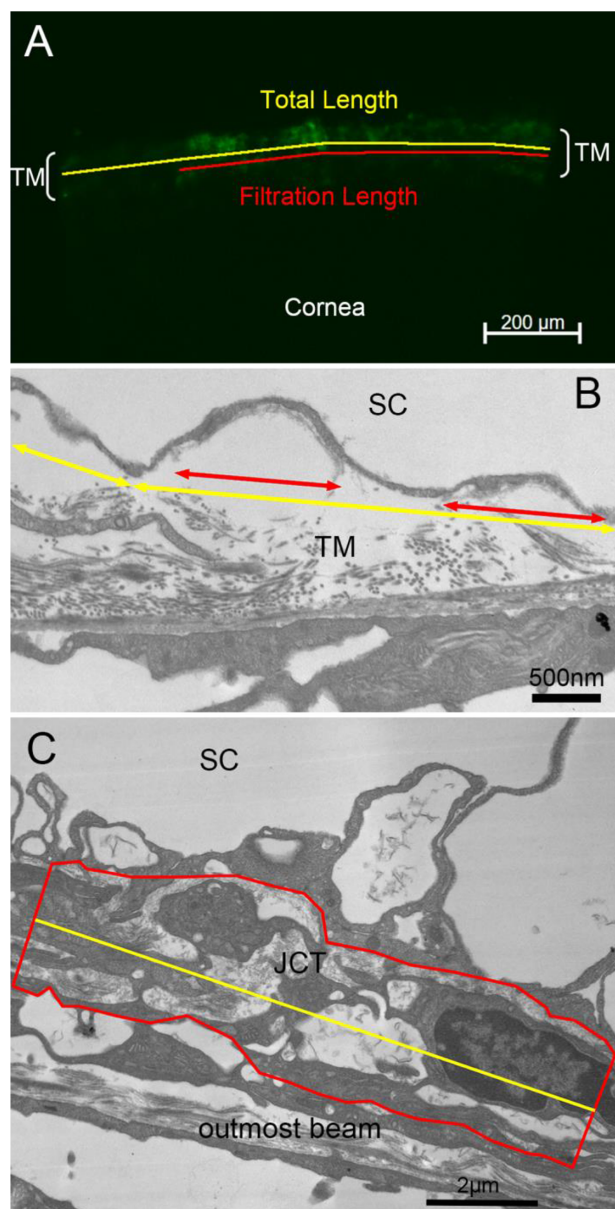


**FIGURE 1. Measurement methods for TM PEFL, PBML, and JCT thickness.** (A) Method of TM PEFL measurements. The tracer distribution is shown in green. The red lines represent effective filtration length (FL) labeled with fluorescent tracers, and the yellow line represents the TL of TM. The average TM PEFL in each perfused mouse eye was calculated as  $\text{TM PEFL} = \frac{\Sigma \text{FL}}{\Sigma \text{TL}} \times 100\%$ . (B) PBML measurements. The yellow double arrows represent the full length of the IW of SC, and the red double arrows represent the BM length.  $\text{PBML} = \frac{\Sigma \text{BM length}}{\Sigma \text{IW length}} \times 100\%$ . (C) Method of JCT thickness measurements. JCT area (red) and JCT length (yellow) were measured. The average JCT thickness ( $\Sigma \text{JCT area} / \Sigma \text{JCT length}$ ) was then calculated accordingly.

ness for each eye was estimated by using TM PEFL as JCT thickness<sub>overall</sub> = JCT thickness<sub>high tracer region</sub> × TM PEFL + JCT thickness<sub>low tracer region</sub> × (1-TM PEFL).

All measurements (including PEFL, PBML, JCT thickness) in this study were repeated by the same investigator (R.R.) once again three months later and by another investigator (A.A.H.) in a masked manner. The difference was less than 6% between the same investigator and less than 8% between different investigators.

### Statistical Analysis

Paired (when comparing to its own baseline IOP) and non-paired (when comparing between different groups) Student's *t*-test and three-way ANOVA were applied for IOP comparison. Mann-Whitney test and Wilcoxon signed rank test were applied for hydrodynamic and morphological comparisons between groups. Linear regression was applied for correlation analyses. All statistical analyses used GraphPad Prism 8 (GraphPad Software, San Diego, CA, USA) with a required significance level of  $P < 0.05$ . All data are shown as mean  $\pm$  SEM.

## RESULTS

### AR-12286 Treatment Reduces IOP in SIOH Mouse Eyes

IOP changes through 5 or 9 weeks are listed in Table 3. Data points from both sexes in each group were combined for analysis since no significant difference was found between male and female mice in DEX-induced IOP increase ( $P = 0.31$ ) or AR-12286 recovered IOP ( $P = 0.98$ ). IOP increased within a week and remained elevated for the following four weeks in all DEX-treated groups compared to the Saline group (Fig. 2A), in which IOP remained unchanged for four weeks and increased  $<1$  mm Hg at week 5 when compared to its own baseline ( $14.8 \pm 0.2$  vs.  $14.1 \pm 0.3$ ,  $P = 0.04$ ). At the end of week 5, IOP of DEX group was  $\sim 6$  mm Hg higher when compared to the Saline group ( $20.9 \pm 0.4$  vs.  $14.8 \pm 0.2$ ,  $P < 0.001$ ). For DEX + AR-12286 group, the IOP increase was similar to DEX group before week 5, then AR-12286 treatment at week 5 reduced IOP by  $\sim 4.5$  mm Hg ( $16.6 \pm 0.5$  vs.  $20.9 \pm 0.4$ ,  $P < 0.001$ ). Although AR-12286 did not fully reverse IOP to the same level as the Saline group ( $P < 0.01$ ), IOP was reduced  $\sim 2$  mm Hg more than in the DEX-DC group at week 5 ( $18.5 \pm 0.6$ ,  $P < 0.05$ ) (Fig. 2A). Detailed IOP changes during week 5 are shown in Table 4 and Figures 2B and C for the Saline, DEX, and DEX + AR12286 groups. AR-12286 reduced the elevated IOP after one day of treatment ( $18.0 \pm 0.5$  vs.  $20.3 \pm 0.4$ ,  $P < 0.01$ ).  $\Delta$ IOP (vs. week 5, day 0) also showed significant negative change at week 5, day 1 ( $P < 0.001$ ). Three-way ANOVA confirmed a significant main effect of the type of treatment (DEX vs. DEX + AR-12286,  $F [1, 40] = 30.42$ ,  $P < 0.0001$ )

**TABLE 3. Comparison of Weekly IOP (mm Hg) Data**

Time	Week 0	Week 1	Week 2	Week 3	Week 4	Week 5
Saline	$14.1 \pm 0.3$	$13.8 \pm 0.3$	$13.8 \pm 0.2$	$13.6 \pm 0.3$	$14.0 \pm 0.3$	$14.8 \pm 0.2$
DEX	$14.2 \pm 0.3$	$18.5 \pm 0.3$	$18.5 \pm 0.4$	$20.7 \pm 0.5$	$20.0 \pm 0.4$	$20.9 \pm 0.4$
DEX + AR-12286	$14.5 \pm 0.3$	$18.7 \pm 0.4$	$20.1 \pm 0.4$	$20.6 \pm 0.5$	$19.7 \pm 0.4$	$16.6 \pm 0.5$
DEX-DC	$12.9 \pm 0.4$	$16.9 \pm 0.5$	$18.7 \pm 0.6$	$20.2 \pm 0.7$	$20.3 \pm 0.6$	$18.5 \pm 0.6$
Time	Week 6	Week 7	Week 8	Week 9		
DEX-DC	$16.5 \pm 0.6$	$15.9 \pm 0.6$	$14.5 \pm 0.5$	$14.3 \pm 0.4$		

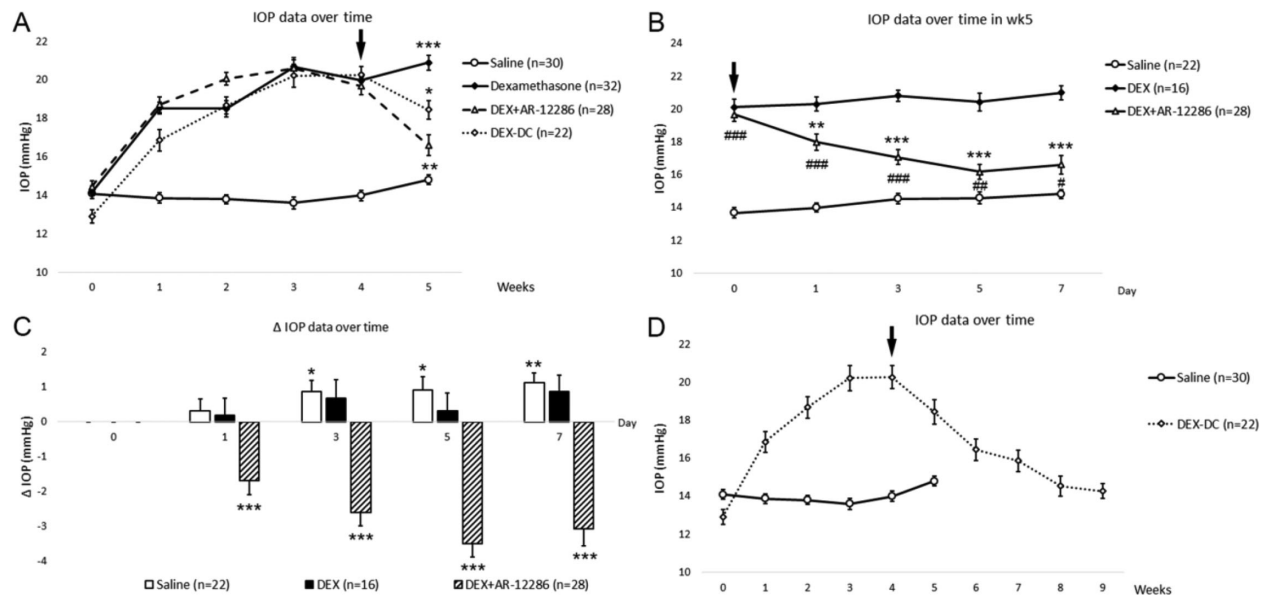


**FIGURE 2. Intraocular pressure (IOP).** (A) IOP measurements through week 5. DEX increased IOP over time. SIOH eyes showed significantly increased IOP at all time-points after treatment. In the DEX + AR-12286 group, IOP changed similarly to the DEX group during the first four weeks, but IOP decreased in the last week with the application of AR-12286. The DEX + AR-12286 group also showed a more significant reduction in IOP when compared to the DEX-DC group. (Asterisk:  $P$  value when compared to IOP of DEX + AR-12286 group at week 5. \* $P < 0.05$ ; \*\* $P < 0.01$ ; \*\*\* $P < 0.001$ ). (B) IOP measurements during week 5. AR-12286 rescued SIOH after one day of treatment. (\* $P$  value when compared to IOP of DEX group; #  $P$  value when compared to IOP of the Saline group). (C)  $\Delta$ IOP (vs. week 5, Day 0) during week 5. AR-12286 reversed IOP change after one day of treatment. \*\*\* $P < 0.001$ . (D) IOP measurements with discontinuation of DEX treatment. Discontinuation of DEX decreased IOP over time and reversed IOP to the similar level of Saline control around week 9. Black arrows indicate the start of application of AR-12286 or DC of DEX.

**TABLE 4.** Detailed IOP (mm Hg) Data in Week 5

Time	Day 0	Day 1	Day 3	Day 5	Day 7
Saline	13.7 $\pm$ 0.3	14.0 $\pm$ 0.3	14.5 $\pm$ 0.3	14.6 $\pm$ 0.4	14.8 $\pm$ 0.3
DEX	20.1 $\pm$ 0.5	20.3 $\pm$ 0.4	20.8 $\pm$ 0.3	20.4 $\pm$ 0.5	21.0 $\pm$ 0.4
DEX + AR-12286	19.7 $\pm$ 0.4	18.0 $\pm$ 0.5	17.1 $\pm$ 0.4	16.2 $\pm$ 0.5	16.6 $\pm$ 0.5

and of time ( $F [3.738, 149.5] = 5.196, P = 0.0008$ ). There was also a significant interaction between the type of treatment and time ( $F [4, 160] = 10.43, P < 0.0001$ ), suggesting that AR-12286 significantly reduced IOP over time. Although the reduction in IOP was not as much as that induced by AR-12286, IOP in the DEX-DC group at the end of week 5 (after one week of discontinuation of DEX treatment) was also significantly lower than in the DEX group ( $P = 0.003$ ). At week 9 (after five weeks of discontinuation of DEX treatment), IOP in the DEX-DC group was at a similar level to the IOP in the Saline group (Table 3, Fig. 2D).

### AR-12286 Treatment Recovers Reduced EFA in SIOH Mouse Eyes

When calculated using en face confocal images, TM PEFL was 48.34%  $\pm$  5.38% in the DEX group ( $n = 11$ ), which was significantly less compared to the Saline group TM PEFL of 72.25%  $\pm$  4.67% ( $n = 11; P = 0.002$ ) (Figs. 3A, 3B). AR-12286 treatment recovered TM PEFL back to 70.44%  $\pm$  5.15%, with a significant increase when compared to the DEX group ( $n = 7; P = 0.02$ ) and similar to the Saline group ( $P = 0.54$ ). At week 9, discontinuation of DEX treatment also increased the TM PEFL to 76.27%  $\pm$  5.01% ( $n = 6$ ), signif-

icantly differed from that in the DEX group at week 5 ( $P = 0.002$ ). There was a significant negative correlation found between TM PEFL and IOP ( $N = 35, R^2 = 0.36, P = 0.0002$ ) (Fig. 3C).

### AR-12286 Treatment Reduces the Increased ECM in SIOH Mouse Eyes

Consistent with our previous report,<sup>38</sup> morphological changes in the ECM of the TM were observed in SIOH eyes, including the increase of deposition of BM-like materials (Fig. 4B), FBM (Fig. 4C), short curly filaments (Fig. 4D), and increased PBML (Figs. 5 and 6). After either one week of AR-12286 treatment or five weeks of discontinuation of DEX treatment, less abnormal ECM was observed in the TM (Table 5). The AR-12286-treated or DEX-DC eyes with abnormal ECM present were found correlated with a relatively higher endpoint IOP as well.

The increased PBML in SIOH eyes, caused by increase of both BM and BM-like materials, was also decreased after AR-12286 treatment (Figs. 5 and 6). In Saline, DEX, and DEX+AR-12286 groups, PBML was greater in low-tracer regions than high-tracer regions (Fig. 6A). PBML in low-tracer versus high-tracer regions was 44.73%  $\pm$  0.06% vs.

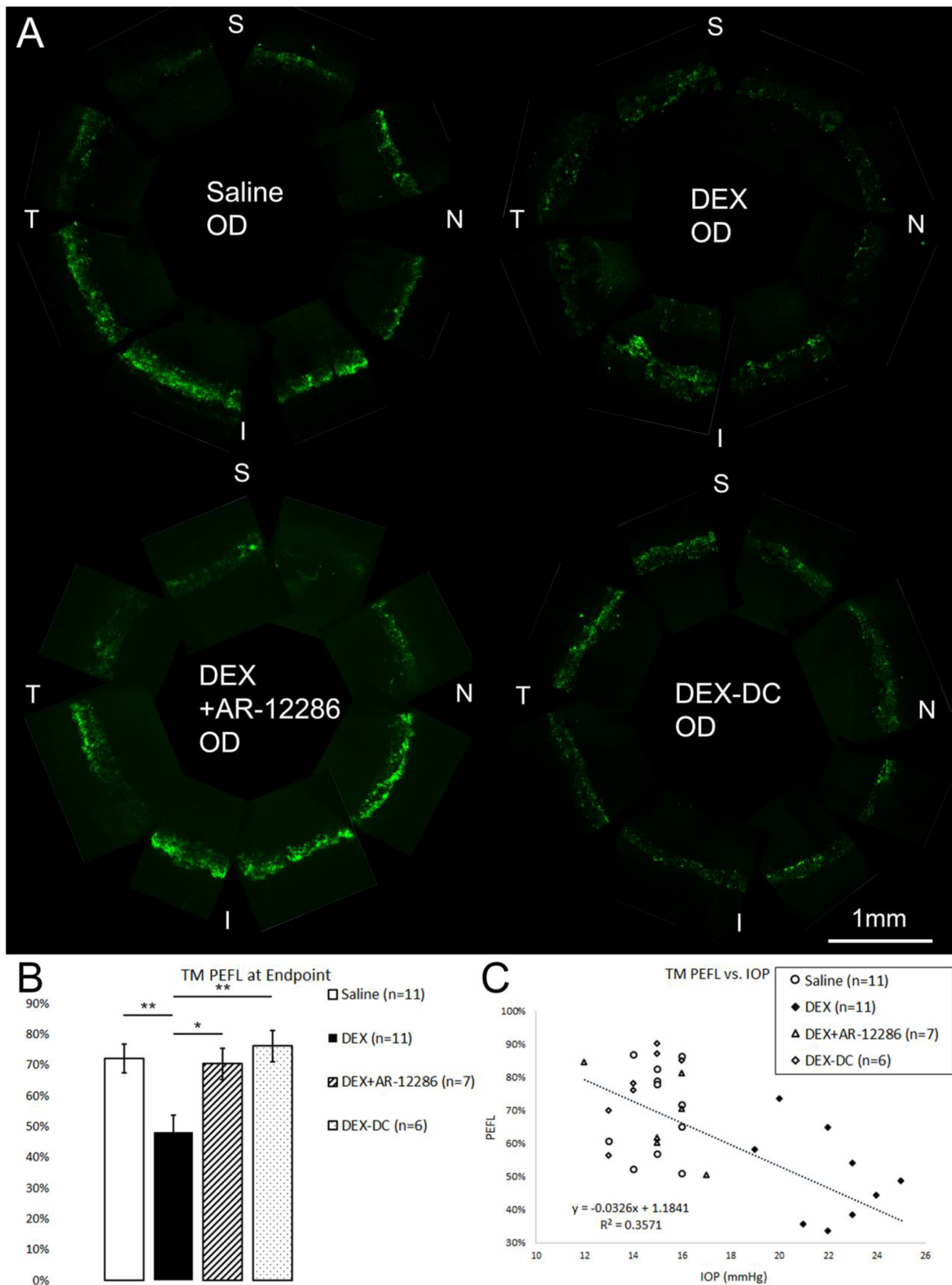


**FIGURE 3. Trabecular meshwork (TM) percentage effective filtration length (PEFL).** (A) Representative en face images of eyes from each group. The tracer distribution is shown in green. (S, superior; N, nasal; I, Inferior; T, temporal). (B) TM PEFL at endpoint. DEX induced a significant reduction in TM PEFL when compared to the Saline group (\*\* $P < 0.01$ ), whereas both AR-12286 (\* $P < 0.05$ ) and DEX-DC (\*\* $P < 0.01$ ) recovered this reduction. (C) TM PEFL-IOP correlation. There was a significant negative correlation between TM PEFL and IOP ( $R^2 = 0.36$ ,  $P < 0.001$ ).

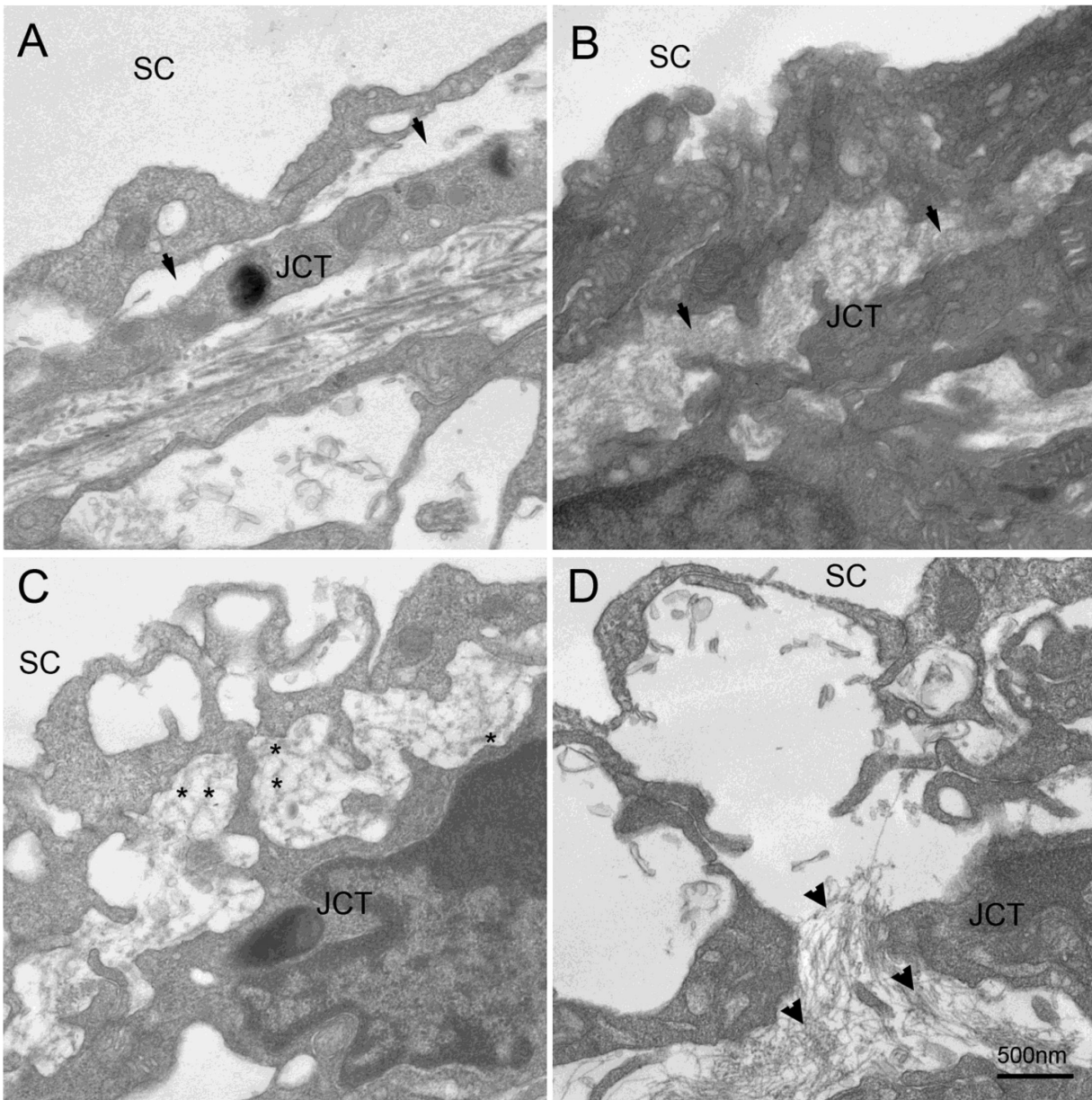


**FIGURE 4. Morphological changes in the ECM of the TM.** (A) Representative electron microscopy (EM) image shows the ultrastructure of the JCT region in control eyes. The space beneath the inner wall of SC (arrows) is almost empty. (B–D) Representative EM images show the ultrastructure of JCT regions in DEX-treated eyes. Increased deposition of basement membrane-like materials in the space beneath the inner wall of SC (arrows) (B), the formation of fingerprint-like arranged materials resembling basement membrane (asterisks) (C), and the formation of short curly filaments (arrowheads) (D) were observed.

28.56%  $\pm$  3.24% in the Saline group ( $P = 0.03$ ), 69.00%  $\pm$  3.85% versus 52.07%  $\pm$  3.10% in the DEX group ( $P = 0.03$ ), and 58.88%  $\pm$  2.48% versus 41.50%  $\pm$  2.44% in the DEX + AR-12286 group ( $P = 0.03$ ), respectively. In DEX-DC group, mean PBML was also greater in low-tracer regions than high-tracer regions (55.64%  $\pm$  2.41% vs. 44.63%  $\pm$  1.11%). However, this difference approached but did not reach statistical significance ( $P = 0.06$ ). PBML was significantly greater than that in the Saline group in both high- and low-tracer regions in DEX (high-tracer regions:  $P = 0.002$ ; low-tracer regions:  $P = 0.002$ ), DEX + AR-12286 (high-tracer regions:  $P = 0.02$ ; low-tracer regions:  $P = 0.002$ ), and DEX-DC groups (high-tracer regions:  $P = 0.004$ ; low-

tracer regions:  $P = 0.009$ ). AR-12286 treatment significantly reduced the DEX-induced increase in PBML in high-tracer regions ( $P = 0.03$ ). There was a significant increase in overall PBML in the DEX ( $P = 0.002$ ), DEX + AR-12286 ( $P = 0.009$ ), and DEX-DC ( $P = 0.004$ ) groups when compared to the Saline group (Fig. 6B). There was a significant reduction in overall PBML in the DEX + AR-12286 ( $P = 0.02$ ) and DEX-DC ( $P = 0.009$ ) groups when compared to the DEX group. There was a significant positive correlation found between overall PBML and IOP ( $N = 17$ ,  $R^2 = 0.49$ ,  $P = 0.0002$ ) (Fig. 6C). There was also a significant negative correlation found between TM PEFL and overall PBML ( $N = 17$ ,  $R^2 = 0.44$ ,  $P = 0.0005$ ) (Fig. 6D).

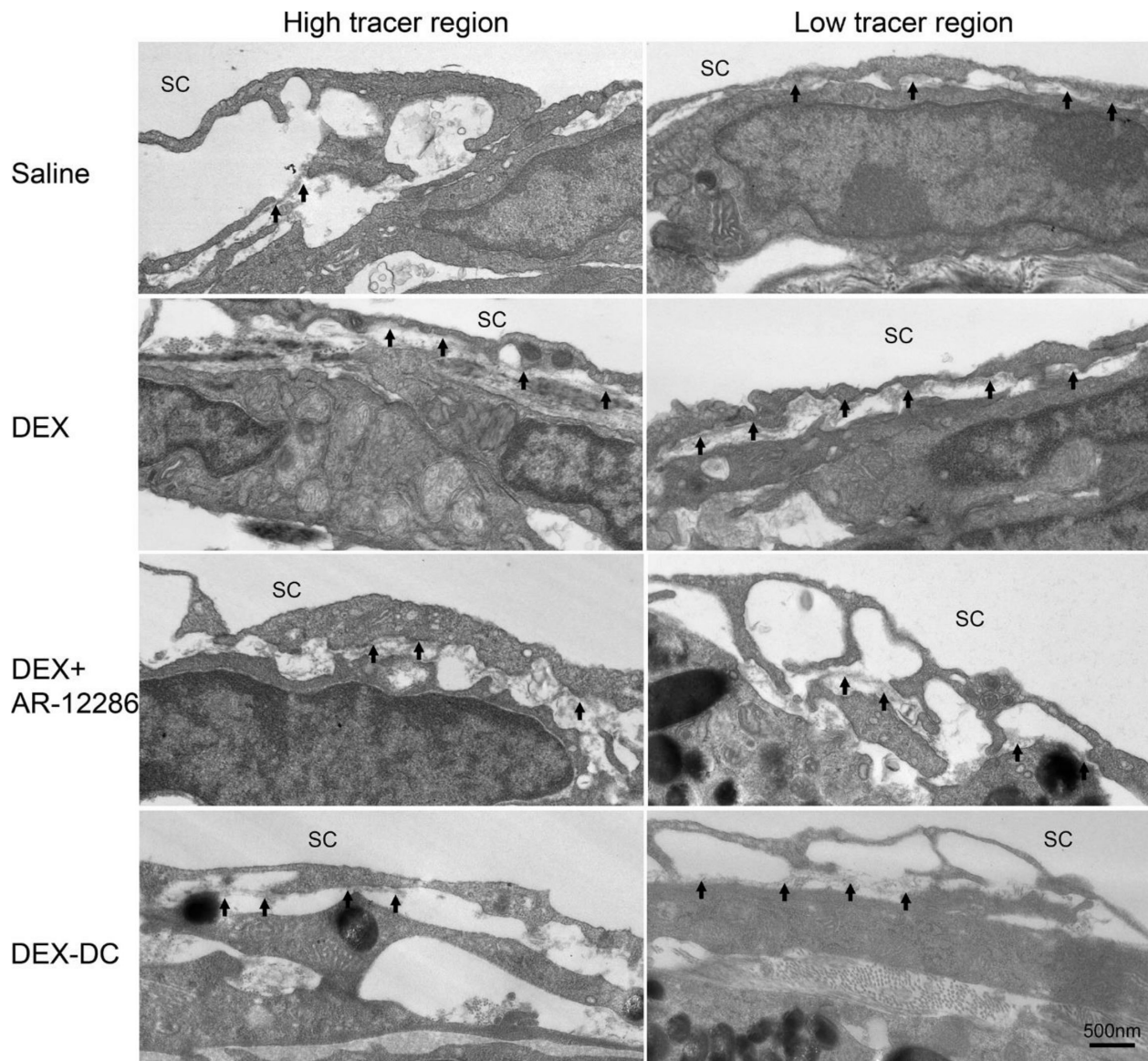


**FIGURE 5. TEM images showing PBML Changes.** Representative electron microscope images around inner wall of SC from high- and low-tracer regions of each group of eyes. The *arrows* indicate BM or BM-like materials.

### AR-12286 Treatment Expanded the Compacted JCT in SIOH Mouse Eyes

Consistent with what we previously reported,<sup>38</sup> in the Saline group, JCT thickness in high-tracer regions was significantly greater than in low-tracer regions ( $3.00 \pm 0.10 \mu\text{m}$  vs.  $2.22 \pm 0.14 \mu\text{m}$ ,  $P = 0.03$ ) (Figs. 7A, 7B). DEX treatment significantly reduced JCT thickness in high-tracer region ( $2.03 \pm 0.11 \mu\text{m}$ ,  $P = 0.002$ ), making it similar to that in low-tracer regions ( $1.82 \pm 0.08 \mu\text{m}$ ,  $P = 0.09$ ). AR-12286 treatment significantly expanded JCT in both high- ( $3.19 \pm 0.15 \mu\text{m}$ ,  $P = 0.002$ ) and low- ( $2.51 \pm 0.16 \mu\text{m}$ ,  $P = 0.004$ ) tracer regions when compared to the DEX group. The JCT thickness in DEX-DC group was significantly greater than that in the DEX group in high-tracer regions ( $3.33 \pm 0.23 \mu\text{m}$ ,  $P = 0.004$ ). The increase in mean JCT thickness in DEX-DC group when compared to the DEX group in low-tracer regions approached but did not reach statistical significance ( $2.41 \pm 0.27 \mu\text{m}$ ,  $P = 0.05$ ).

There was a significant reduction in JCT thickness in the DEX group when compared to the Saline group ( $1.77 \pm 0.06 \mu\text{m}$  vs.  $2.75 \pm 0.14 \mu\text{m}$ ,  $P = 0.002$ ) (Fig. 7C). There was a significant increase in JCT thickness in DEX + AR-12286 ( $2.97 \pm 0.11 \mu\text{m}$ ,  $P = 0.002$ ) and DEX-DC ( $3.12 \pm 0.20 \mu\text{m}$ ,  $P = 0.004$ ) group when compared to DEX group.

### DISCUSSION

In this study, we investigated whether the ROCK inhibitor AR-12286 could rescue SIOH and offset the DEX-induced hydrodynamic and morphologic changes in the trabecular outflow pathway, and we compared the effects of AR-12286 with discontinuation of steroid administration. To the best of our knowledge, this is the first quantitative study of hydrodynamic and morphological changes induced in SIOH mouse eyes by a highly selective Rho kinase inhibitor, and the first study to compare the changes in the trabecular outflow path-

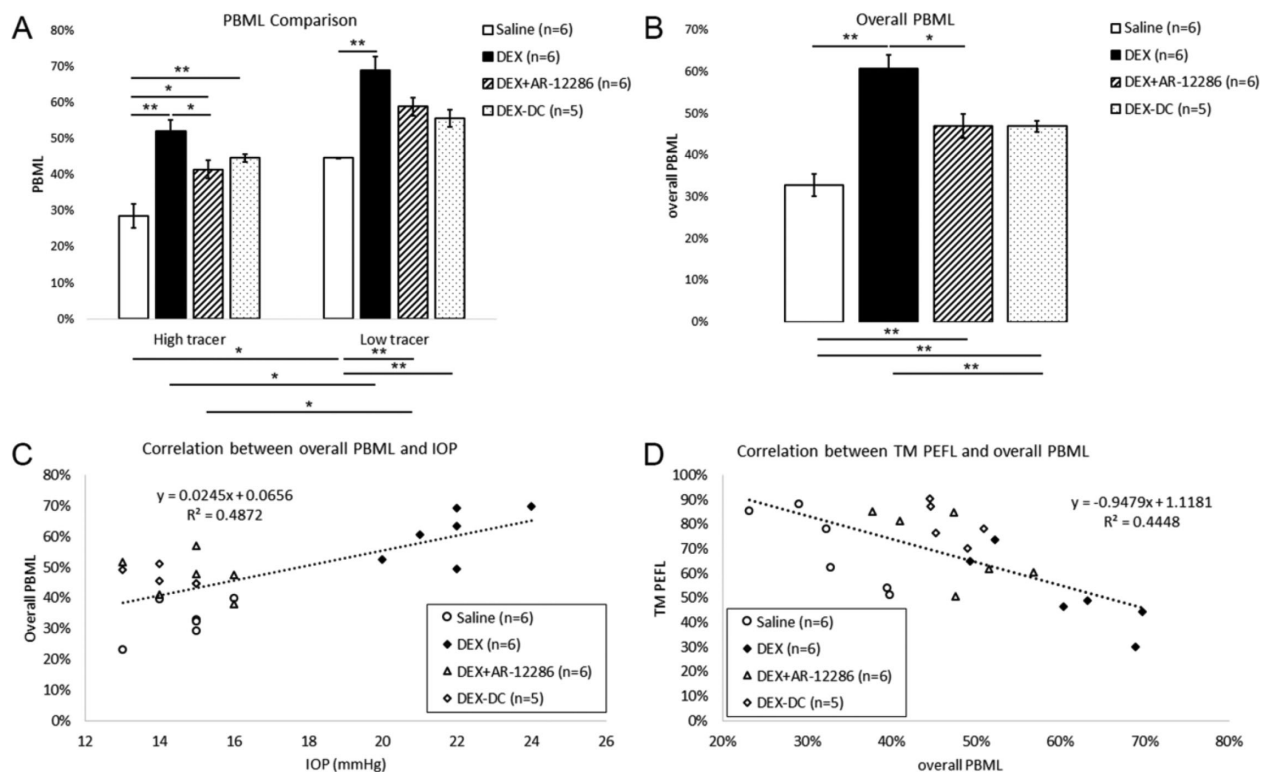


**FIGURE 6. Percentage basement membrane length (PBML) comparison.** (A) In the Saline, DEX, and DEX + AR-12286 groups, PBML is significantly greater in low-tracer regions compared to high-tracer region ( $*P < 0.05$ ). DEX treatment induced a significant increase in PBML in both high- and low-tracer regions compared to the Saline controls ( $**P < 0.01$ ). After AR-12286 treatment or DC of DEX, this increase in PBML became nonsignificant in low-tracer regions, although it remains significant in high-tracer regions ( $*P < 0.05$ ;  $**P < 0.01$ ). However, AR-12286 induced a significant reduction in PBML in high-tracer regions when compared to the DEX group ( $*P < 0.05$ ). (B) The overall PBML was significantly increased in all DEX-treated eyes when compared to Saline controls ( $**P < 0.01$ ). Both AR-12286 and DC of DEX significantly reduced overall PBML when compared to DEX group ( $*P < 0.05$ ;  $**P < 0.01$ ). (C) There was a significant positive correlation between IOP and overall PBML ( $R^2 = 0.49$ ,  $P = 0.0002$ ). (D) There was a significant negative correlation between TM PEFL and overall PBML ( $R^2 = 0.44$ ,  $P = 0.0005$ ).

**TABLE 5. Presence of Abnormal ECM in the TM**

Group	BM-Like Materials	FBM	Short Curly Filaments
Saline	1 out of 6 eyes	0 out of 6 eyes	1 out of 6 eyes
DEX	6 out of 6 eyes	4 out of 6 eyes	3 out of 6 eyes
DEX + AR-12286	2 out of 6 eyes	1 out of 6 eyes	2 out of 6 eyes
DEX-DC	1 out of 5 eyes	0 out of 5 eyes	2 out of 5 eyes

way to the discontinuation of steroid treatment. The topical application of AR-12286 decreased IOP in SIOH mouse eyes within a week by increasing EFA in the TM. Morphological correlations with this increased EFA included expansion of the JCT in both high- and low-tracer regions and decreased deposition of ECM in the TM. Our data suggested that even when accompanied with continuous topical steroid treatment, AR-12286 reduced IOP in SIOH eyes more effectively than the discontinuation of DEX treatment. The hydrodynamic and morphological changes caused by AR-12286 on SIOH eyes within a week were similar to those caused by discontinuation of DEX treatment for five weeks. Therefore there is a potential for using AR-12286 to lower SIOH in patients who rely on steroid treatment.

Similar to a previous study which investigated the effects of Rho kinase inhibitor netarsudil on SIOH mouse eyes,<sup>45</sup> we observed a significant reduction of IOP after one day of AR-12286 treatment, which was followed by a contin-

uous decrease in IOP over one week. While netarsudil was reported to produce ~50% reduction of IOP after four days of treatment of SIOH mouse eyes, we found AR-12286 produced ~60% to 70% reduction of IOP after 3 or 5 days of treatment (Day 3 or Day 5 of week 5 in Table 4). Consistent with the reported reversal of steroid-induced reduction in outflow facility by netarsudil,<sup>45</sup> we observed a reversal of the steroid-induced reduction in active filtration area by AR-12286 that was similar to discontinuation of steroid treatment. Just as a previous study<sup>51</sup> found a negative correlation between IOP and outflow facility, we found a negative correlation between IOP and PEFL, which is consistent with our previous findings in SIOH and normal mouse eyes.<sup>38</sup> However, although retrospective cohort studies of netarsudil and another Rho kinase inhibitor glaucoma medication, ripasudil, have reported success in lowering IOP in steroid-induced glaucoma patients,<sup>45-57</sup> another retrospective study with a smaller sample size found no significant reduction in

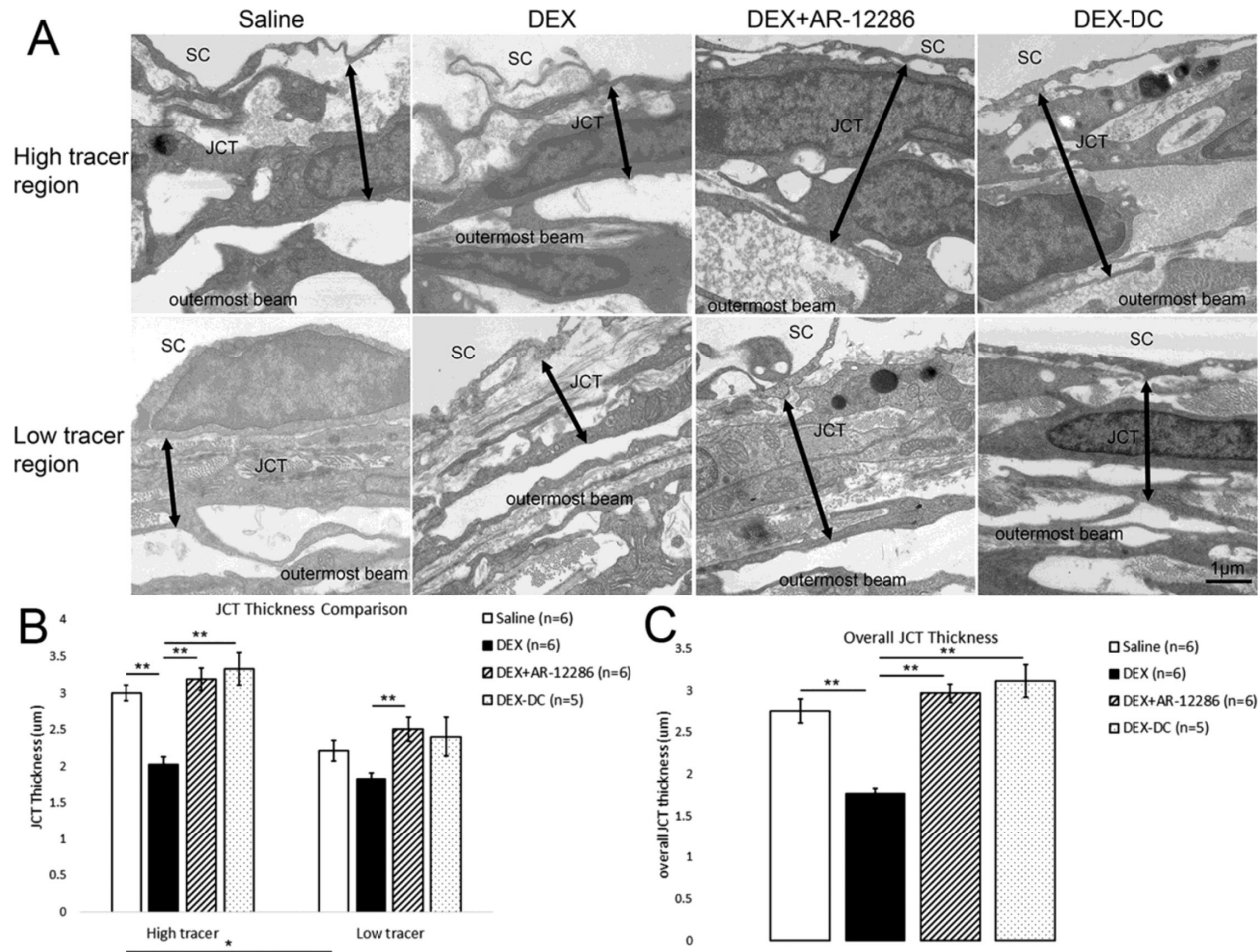


**FIGURE 7. JCT thickness.** (A) Representative electron microscopy images of JCT from high and low-tracer regions of each group of eyes. Double arrows represent the JCT thickness. (B) A more expanded JCT was found in high-tracer regions than low-tracer regions in the Saline group ( $*P < 0.05$ ). DEX treatment significantly reduced JCT thickness in high-tracer regions compared to high-tracer regions in the Saline group ( $**P < 0.01$ ). AR-12286 treatment significantly expanded JCT in both high- and low-tracer regions when compared to DEX group ( $**P < 0.01$ ). DC of DEX significantly expanded JCT in high-tracer regions when compared to DEX group ( $**P < 0.01$ ). (C) The overall JCT thickness was significantly decreased in DEX-treated group when compared to the Saline controls ( $**P < 0.01$ ). Both AR-12286 treatment and DC of DEX significantly increased overall JCT thickness when compared to the DEX group ( $**P < 0.01$ ).

IOP in steroid-induced glaucoma patients, whereas significant reduction was found in POAG patients.<sup>58</sup>

Also consistent with the findings of reversed steroid-induced increase in TM stiffness and fibrotic markers in the previous study with netarsudil,<sup>45</sup> we found that AR-12286 treatment reversed the steroid-induced compacted JCT and steroid-induced increase in the ECM deposition in the TM. Consistent with our previous study in SIOH and normal mouse eyes,<sup>38</sup> we found a positive correlation between PBML and PEFL and a negative correlation between PBML and IOP. However, although one week of AR-12286 treatment and five weeks of DC of DEX treatment both reversed PEFL and JCT thickness to a similar level, they only partially reversed PBML, and their IOP was significantly different from each other. This suggests that although one week of AR-12286 treatment could offset the steroid-induced changes in the trabecular outflow pathway to a similar level as five weeks DC of DEX, a longer DC of DEX may result in further reduction of IOP via other unknown mechanisms.

We found that Rho kinase inhibitor AR-12286 induced a decrease in ECM deposition, especially in the JCT region. The previous study with netarsudil suggested that this reduc-

tion in ECM deposition may be related to the anti-fibrotic activity of Rho kinase inhibition.<sup>45</sup> Other studies with 2D and 3D human trabecular meshwork cell culture also suggest that Rho kinase inhibitors can reverse the steroid-induced upregulation in ECM components and downregulation in matrix metalloproteinases.<sup>59,60</sup> However, further studies are needed to better understand the mechanisms associated with the anti-fibrotic activity of Rho kinase inhibitors.

Interestingly, we found that there was a greater increase in the IOP of DEX-treated mouse eyes when the interval time between two doses of DEX was decreased. In our previous quantitative study on DEX-induced hydrodynamic and morphological changes on mouse eyes,<sup>38</sup> the interval between two daily doses of DEX was eight hours (first dose at 9–11 AM and second dose at 5–7 PM). However, in the current study, to add two daily doses of AR-12286, the interval between two daily doses of DEX was reduced from eight hours to 6.5 hours (first dose at 8–10 AM and second dose at 2:30–4:30 PM). The IOP in DEX-treated mouse eyes in our current study versus previous study was  $14.2 \pm 0.3$  versus  $13.8 \pm 0.4$  mm Hg at baseline ( $P = 0.54$ , two-tailed, non-paired *t*-test),  $18.5 \pm 0.3$  vs.  $16.5 \pm 0.6$  ( $P = 0.004$ ) after

week 1 of treatment,  $18.5 \pm 0.4$  versus  $16.9 \pm 0.4$  ( $P = 0.005$ ) at week 2,  $20.7 \pm 0.5$  versus  $17.7 \pm 0.5$  ( $P = 0.0001$ ) at week 3,  $20.0 \pm 0.4$  versus  $17.8 \pm 0.4$  ( $P = 0.0003$ ) at week 4, and  $20.9 \pm 0.4$  versus  $17.9 \pm 0.4$  ( $P < 0.0001$ ) at week 5. These data suggest that a shorter interval between two doses of DEX may induce a booster effect and result in a greater IOP elevation in mouse eyes. However, although there was a small reduction in the average of TM PEFL in the DEX-treated mouse eyes in current study when compared to our previous study ( $48.34\% \pm 5.38\%$  vs.  $50.89\% \pm 4.52\%$ ), this reduction did not reach statistical significance ( $P = 0.78$ , Mann Whitney test). There was also no significant difference found between overall JCT thickness ( $1.77 \pm 0.06 \mu\text{m}$  vs.  $1.80 \pm 0.18 \mu\text{m}$ ,  $P = 0.93$ ) or overall PBML ( $60.68\% \pm 3.44\%$  vs.  $63.18\% \pm 3.45\%$ ,  $P = 0.75$ ). These findings suggest that the booster effect on IOP caused by shorter interval DEX dosing may not be induced by the hydrodynamic and morphological changes in the trabecular outflow pathway. Other possible mechanisms, such as changes in aqueous humor production or uveal outflow may need to be investigated.

In summary, by using an SIOH mouse model, we have shown that the highly selective Rho kinase inhibitor AR-12286 lowers IOP in one week via reversing steroid-induced hydrodynamic and morphological changes in the trabecular meshwork of ocular hypertensive mouse eyes. AR-12286 expands the compacted trabecular meshwork, reduces the increased abnormal extracellular matrix, reduces the elevated inner wall endothelial basement membrane continuity, and results in an increase in active filtration area, consequently lowering IOP. Rho kinase inhibitor AR-12286 can reduce steroid-induced IOP elevation more effectively than a five-week DC of steroid treatment. These results suggest that Rho kinase inhibitors hold promise as a therapeutic option for lowering IOP in patients who rely on steroid treatment.

### Acknowledgments

Supported by Aerie Pharmaceuticals, Inc., NIH EY022634, and the Massachusetts Lions Eye Research Fund.

Disclosure: **R. Ren**, Aerie (F); **A.A. Humphrey**, None; **C. Kopczyński**, Aerie (E); **H. Gong**, Aerie (F)

### References

- McMonnies CW. Intraocular pressure spikes in keratectasia, axial myopia, and glaucoma. *Optom Vis Sci.* 2008;85:1018–1026.
- Grant WM. Experimental aqueous perfusion in enucleated human eyes. *Arch Ophthalmol.* 1963;69:783–801.
- Heijl A, Leske MC, Bengtsson B, et al. Reduction of intraocular pressure and glaucoma progression: results from the Early Manifest Glaucoma Trial. *Arch Ophthalmol.* 2002;120:1268–1279.
- Leske MC, Heijl A, Hyman L, et al. Predictors of long-term progression in the early manifest glaucoma trial. *Ophthalmology.* 2007;114:1965–1972.
- Gordon MO, Beiser JA, Brandt JD, et al. The Ocular Hypertension Treatment Study: baseline factors that predict the onset of primary open-angle glaucoma. *Arch Ophthalmol.* 2002;120:714–720; discussion 829–830.
- Kass MA, Heuer DK, Higginbotham EJ, et al. The Ocular Hypertension Treatment Study: a randomized trial determines that topical ocular hypotensive medication delays or prevents the onset of primary open-angle glaucoma. *Arch Ophthalmol.* 2002;120:701–713; discussion 829–830.
- Collaborative Normal-Tension Glaucoma Study Group. Comparison of glaucomatous progression between untreated patients with normal-tension glaucoma and patients with therapeutically reduced intraocular pressures. *Am J Ophthalmol.* 1998;126:487–497.
- The AGIS Investigators. The Advanced Glaucoma Intervention Study (AGIS): 7. The relationship between control of intraocular pressure and visual field deterioration. *Am J Ophthalmol.* 2000;130:429–440.
- Fiscella RG, Lesar TS, Edward DP. *Pharmacotherapy A Pathophysiologic Approach.* 9th ed. New York: McGraw-Hill Education/Medical; 2014.
- Marquis RE, Whitson JT. Management of glaucoma: focus on pharmacological therapy. *Drugs Aging.* 2005;22:1–21.
- Sumida GM, Stamer WD. Sphingosine-1-phosphate enhancement of cortical actomyosin organization in cultured human Schlemm's canal endothelial cell monolayers. *Invest Ophthalmol Vis Sci.* 2010;51:6633–6638.
- Ramos RF, Sumida GM, Stamer WD. Cyclic mechanical stress and trabecular meshwork cell contractility. *Invest Ophthalmol Vis Sci.* 2009;50:3826–3832.
- WuDunn D. Mechanobiology of trabecular meshwork cells. *Exp Eye Res.* 2009;88:718–723.
- Zhang M, Maddala R, Rao PV. Novel molecular insights into RhoA GTPase-induced resistance to aqueous humor outflow through the trabecular meshwork. *Am J Physiol Cell Physiol.* 2008;295:C1057–C1070.
- Faralli JA, Newman JR, Sheibani N, Dedhar S, Peters DM. Integrin-linked kinase regulates integrin signaling in human trabecular meshwork cells. *Invest Ophthalmol Vis Sci.* 2011;52:1684–1692.
- Schwinn MK, Gonzalez JM, Gabelt BT, Sheibani N, Kaufman PL, Peters DM. Heparin II domain of fibronectin mediates contractility through an alpha4beta1 co-signaling pathway. *Exp Cell Res.* 2010;316:1500–1512.
- Rao PV, Deng PF, Kumar J, Epstein DL. Modulation of aqueous humor outflow facility by the Rho kinase-specific inhibitor Y-27632. *Invest Ophthalmol Vis Sci.* 2001;42:1029–1037.
- Aga M, Bradley JM, Keller KE, Kelley MJ, Acott TS. Specialized podosome- or invadopodia-like structures (PILS) for focal trabecular meshwork extracellular matrix turnover. *Invest Ophthalmol Vis Sci.* 2008;49:5353–5365.
- Mäepea O, Bill A. Pressures in the juxtacanalicular tissue and Schlemm's canal in monkeys. *Exp Eye Res.* 1992;54:879–883.
- Mäepea O, Bill A. The pressures in the episcleral veins, Schlemm's canal and the trabecular meshwork in monkeys: effects of changes in intraocular pressure. *Exp Eye Res.* 1989;49:645–663.
- Johnson M, Shapiro A, Ethier CR, Kamm RD. Modulation of outflow resistance by the pores of the inner wall endothelium. *Invest Ophthalmol Vis Sci.* 1992;33:1670–1675.
- Vahabikashi A, Gelman A, Dong B, et al. Increased stiffness and flow resistance of the inner wall of Schlemm's canal in glaucomatous human eyes. *Proc Natl Acad Sci USA.* 2019;116:26555–26563.
- Battista SA, Lu Z, Hofmann S, Freddo T, Overby DR, Gong H. Reduction of the available area for aqueous humor outflow and increase in meshwork herniations into collector channels following acute IOP elevation in bovine eyes. *Invest Ophthalmol Vis Sci.* 2008;49:5346–5352.
- Lu Z, Overby DR, Scott PA, Freddo TF, Gong H. The mechanism of increasing outflow facility by Rho-kinase inhibition with Y-27632 in bovine eyes. *Exp Eye Res.* 2008;86:271–281.
- Scott PA, Lu Z, Liu Y, Gong H. Relationships between increased aqueous outflow facility during washout with

- the changes in hydrodynamic pattern and morphology in bovine aqueous outflow pathways. *Exp Eye Res.* 2009;89:942–949.
26. Zhu J, Ye W, Gong H. Development of a novel two color tracer perfusion technique for the hydrodynamic study of aqueous outflow in bovine eyes. *Chin Med J.* 2010;123:599–605.
  27. Lu Z, Zhang Y, Freddo TF, Gong H. Similar hydrodynamic and morphological changes in the aqueous humor outflow pathway after washout and Y27632 treatment in monkey eyes. *Exp Eye Res.* 2011;93:397–404.
  28. Yang CYC, Liu Y, Lu Z, Ren R, Gong H. Effects of Y27632 on aqueous humor outflow facility with changes in hydrodynamic pattern and morphology in human eyes. *Invest Ophthalmol Vis Sci.* 2013;54:5859–5870.
  29. Cha EDK, Xu J, Gong L, Gong H. Variations in active outflow along the trabecular outflow pathway. *Exp Eye Res.* 2016;146:354–360.
  30. Li G, Mukherjee D, Navarro I, et al. Visualization of conventional outflow tissue responses to netarsudil in living mouse eyes. *Eur J Pharmacol.* 2016;787:20–31.
  31. Braakman ST, Read AT, Chan DWH, Ethier CR, Overby DR. Colocalization of outflow segmentation and pores along the inner wall of Schlemm's canal. *Exp Eye Res.* 2015;130:87–96.
  32. Chang JYH, Folz SJ, Laryea SN, Overby DR. Multi-scale analysis of segmental outflow patterns in human trabecular meshwork with changing intraocular pressure. *J Ocul Pharmacol Ther.* 2014;30(2-3):213–223.
  33. Keller KE, Bradley JM, Vranka JA, Acott TS. Segmental versican expression in the trabecular meshwork and involvement in outflow facility. *Invest Ophthalmol Vis Sci.* 2011;52:5049–5057.
  34. Vranka JA, Staverosky JA, Raghunathan V, Acott TS. Elevated pressure influences relative distribution of segmental regions of the trabecular meshwork. *Exp Eye Res.* 2020;190:107888.
  35. Lu Z, Zhang Y, Freddo TF, Gong H. Similar hydrodynamic and morphological changes in the aqueous humor outflow pathway after washout and Y27632 treatment in monkey eyes. *Exp Eye Res.* 2011;93:397–404.
  36. Ren R, Li G, Le TD, Kopczynski C, Stamer WD, Gong H. Netarsudil increases outflow facility in human eyes through multiple mechanisms. *Invest Ophthalmol Vis Sci.* 2016;57:6197–6209.
  37. Swaminathan SS, Oh DJ, Kang MH, et al. Secreted protein acidic and rich in cysteine (SPARC)-null mice exhibit more uniform outflow. *Invest Ophthalmol Vis Sci.* 2013;54:2035–2047.
  38. Ren R, Humphrey AA, Swain DL, Gong H. Relationships between intraocular pressure, effective filtration area, and morphological changes in the trabecular meshwork of steroid-induced ocular hypertensive mouse eyes. *Int J Mol Sci.* 2022;23(2):854.
  39. Pattabiraman PP, Epstein DL, Rao PV. Regulation of adherens junctions in trabecular meshwork cells by Rac GTPase and their influence on intraocular pressure. *J Ocul Biol.* 2013;1(1):0002
  40. Pattabiraman PP, Maddala R, Rao PV. Regulation of plasticity and fibrogenic activity of trabecular meshwork cells by Rho GTPase signaling. *J Cell Physiol.* 2014;229:927–942.
  41. Honjo M, Inatani M, Kido N, et al. Effects of protein kinase inhibitor, HA1077, on intraocular pressure and outflow facility in rabbit eyes. *Arch Ophthalmol.* 2001;119:1171–1178.
  42. Honjo M, Tanihara H, Inatani M, et al. Effects of Rho-associated protein kinase inhibitor Y-27632 on intraocular pressure and outflow facility. *Invest Ophthalmol Vis Sci.* 2001;42:137–144.
  43. Kiel JW, Kopczynski CC. Effect of AR-13324 on episcleral venous pressure in Dutch belted rabbits. *J Ocul Pharmacol Ther.* 2015;31:146–151.
  44. Kazemi A, McLaren JW, Kopczynski CC, Heah TG, Novack GD, Sit AJ. The effects of netarsudil ophthalmic solution on aqueous humor dynamics in a randomized study in humans. *J Ocul Pharmacol Ther.* 2018;34:380–386.
  45. Li G, Lee C, Read AT, et al. Anti-fibrotic activity of a Rho-kinase inhibitor restores outflow function and intraocular pressure homeostasis. *eLife.* 2021;10:e60831.
  46. Li G, Lee C, Agrahari V, et al. In vivo measurement of trabecular meshwork stiffness in a corticosteroid-induced ocular hypertensive mouse model. *Proc Natl Acad Sci U S A.* 2019;116:1714–1722.
  47. Johnson D, Gottanka J, Flügel C, Hoffmann F, Futa R, Lütjen-Drecoll E. Ultrastructural changes in the trabecular meshwork of human eyes treated with corticosteroids. *Arch Ophthalmol.* 1997;115:375–383.
  48. Rohen JW, Linnér E, Witmer R. Electron microscopic studies on the trabecular meshwork in two cases of corticosteroid-glaucoma. *Exp Eye Res.* 1973;17:19–31.
  49. Tektas OY, Lütjen-Drecoll E. Structural changes of the trabecular meshwork in different kinds of glaucoma. *Exp Eye Res.* 2009;88:769–775.
  50. Tektas OY, Hammer CM, Danias J, et al. Morphologic changes in the outflow pathways of bovine eyes treated with corticosteroids. *Invest Ophthalmol Vis Sci.* 2010;51:4060–4066.
  51. Overby DR, Bertrand J, Tektas OY, et al. Ultrastructural changes associated with dexamethasone-induced ocular hypertension in mice. *Invest Ophthalmol Vis Sci.* 2014;55:4922–4933.
  52. Lin CW, Sherman B, Moore LA, et al. Discovery and preclinical development of netarsudil, a novel ocular hypotensive agent for the treatment of glaucoma. *J Ocul Pharmacol Ther.* 2018;34(1-2):40–51.
  53. Sturdivant JM, Royalty SM, Lin CW, et al. Discovery of the ROCK inhibitor netarsudil for the treatment of open-angle glaucoma. *Bioorg Med Chem Lett.* 2016;26:2475–2480.
  54. Skaat A, Jasien JV, Ritch R. Efficacy of topically administered Rho-kinase inhibitor AR-12286 in patients with exfoliation syndrome and ocular hypertension or glaucoma. *J Glaucoma.* 2016;25(9):e807–e814.
  55. Williams RD, Novack GD, van Haarlem T, Kopczynski C, AR-12286 Phase 2A Study Group. Ocular hypotensive effect of the Rho kinase inhibitor AR-12286 in patients with glaucoma and ocular hypertension. *Am J Ophthalmol.* 2011;152:834–841.
  56. Zode GS, Sharma AB, Lin X, et al. Ocular-specific ER stress reduction rescues glaucoma in murine glucocorticoid-induced glaucoma. *J Clin Invest.* 2014;124:1956–1965.
  57. Futakuchi A, Morimoto T, Ikeda Y, Tanihara H, Inoue T, ROCK-S study group collaborators. Intraocular pressure-lowering effects of ripasudil in uveitic glaucoma, exfoliation glaucoma, and steroid-induced glaucoma patients: ROCK-S, a multicentre historical cohort study. *Sci Rep.* 2020;10(1):10308.
  58. Kaneko Y, Ohta M, Isobe T, Nakamura Y, Mizuno K. Additive intraocular pressure-lowering effects of ripasudil with glaucoma therapeutic agents in rabbits and monkeys. *J Ophthalmol.* 2017;2017:7079645.
  59. Watanabe M, Ida Y, Furuhashi M, Tsugeno Y, Hikage F, Ohguro H. Pan-ROCK and ROCK2 inhibitors affect dexamethasone-treated 2D- and 3D-cultured human trabecular meshwork (HTM) cells in opposite manners. *Mol Basel Switz.* 2021;26(21):6382.
  60. Li H, Bagué T, Kirschner A, et al. A tissue-engineered human trabecular meshwork hydrogel for advanced glaucoma disease modeling. *Exp Eye Res.* 2021;205:108472.